Fourfold Differential Photoelectron Circular Dichroism

K. Fehre,[1,*] N. M. Novikovskiy,[2,3] S. Grundmann,[1] G. Kastirke,[1] S. Eckart,[1] F. Trinter,[1,4] J. Rist,[1] A. Hartung,[1]
D. Trabert,[1] C. Janke,[1] G. Nalin,[1] M. Pitzer,[1] S. Zeller,[1] F. Wiegandt,[1] M. Weller,[1] M. Kircher,[1] M. Hofmann,[1]
L. Ph. H. Schmidt,[1] A. Knie,[2] A. Hans,[2] L. Ben Ltaief,[5] A. Ehresmann,[2] R. Berger,[6] H. Fukuzawa,[7] K. Ueda,[7]
H. Schmidt-Böcking,[1] J. B. Williams,[8] T. Jahnke,[9] R. Dörner,[1] M. S. Schöffler,[1,†] and Ph. V. Demekhin[2,‡]

[1]*Institut für Kernphysik, Goethe-Universität, Max-von-Laue-Strasse 1, Frankfurt am Main 60438, Germany*
[2]*Institut für Physik und CINSaT, Universität Kassel, Heinrich-Plett-Strasse 40, Kassel 34132, Germany*
[3]*Institute of Physics, Southern Federal University, Rostov-on-Don 344090, Russia*
[4]*Molecular Physics, Fritz-Haber-Institut der Max-Planck-Gesellschaft, Faradayweg 4-6, Berlin 14195, Germany*
[5]*Department of Physics and Astronomy, Aarhus University, Århus 8000, Denmark*
[6]*Theoretical Chemistry, Universität Marburg, Hans-Meerwein-Strasse 4, Marburg 35032, Germany*
[7]*Institute of multidisciplinary research for advanced materials, Tohoku University, Sendai 980-8577, Japan*
[8]*Department of Physics, University of Nevada, Reno, Nevada 89557, USA*
[9]*European XFEL, Holzkoppel 4, Schenefeld 22869, Germany*

We report on a joint experimental and theoretical study of photoelectron circular dichroism (PECD) in methyloxirane. By detecting O 1s photoelectrons in coincidence with fragment ions, we deduce the molecule's orientation and photoelectron emission direction in the laboratory frame. Thereby, we retrieve a fourfold differential PECD clearly beyond 50%. This strong chiral asymmetry is reproduced by *ab initio* electronic structure calculations. Providing such a pronounced contrast makes PECD of fixed-in-space chiral molecules an even more sensitive tool for chiral recognition in the gas phase.

The interaction of chiral matter with circularly polarized light depends on the light's helicity, giving rise to so-called chiroptical effects. Scalar observables, such as circular dichroism (CD, [1]), rely on the interference between the electric-dipole and magnetic-dipole light-matter interactions. Accordingly, the magnitude of the effect is typically very small, i.e., on the order of 10^{-6}–10^{-3} of the total absorption. Because of such rather weak contrast, this chiroptical effect is routinely utilized for chiral recognition mainly in the condensed phase [2]. A pioneering theoretical prediction [3] of a substantial forward-backward asymmetry in the laboratory-frame angular distributions of photoelectrons emitted from randomly oriented chiral molecules (and a later experimental verification of this effect [4]) paved the way for establishing a new tool for chiral recognition in the gas phase. Because this effect, known as photoelectron circular dichroism (PECD, [5–7]), relies purely on the electric-dipole light-matter interaction, it is much stronger than the conventional CD. Its strength typically reaches a few percent. PECD is a universal chiroptical effect [8] persisting in many regimes: one-photon ionization [5–7], resonance-enhanced multiphoton ionization [9,10], above-threshold ionization [8,11], strong-field ionization [8,12], and multiphoton ionization by bichromatic fields [13–16]. Because of its high contrast as compared to the conventional CD, PECD became a well-established tool for enantiomeric excess determination in the gas phase with a subpercent resolution [17].

Obviously, further improving the sensitivity of the enantiomeric excess determination by means of PECD would require a considerable increase of its strength. But what are the limits of PECD and how can it be enhanced [18]? One of the discussed routes is to utilize a coherent control scheme to optimize the light properties, which may increase the chiral response up to about 68% [19] (which corresponds to about 34% for the normalized difference discussed in this work). Alternatively, since PECD of randomly oriented molecules is just a small fraction of a nonaveraged chiral response [3] and, thus, the averaging over different molecular orientations inevitably leads to a loss of information, it is a viable route to increase the observed effect by fixing the target molecules in space. For diatomic (and thus achiral) molecules, this strategy yields up to 100% circular dichroism in the angular distribution (CDAD, [20,21]). The CDAD effect is, however, confined in the polarization plane of the circularly polarized light (i.e., it occurs without establishing a forward-backward asymmetry as in the PECD [22]). Our theoretical predictions [23] illustrate that fixing the molecular orientation in all three spatial dimensions may also result in a PECD of 100%. In this previous study [23] on methyloxirane (C_3H_6O) and in the subsequent study [24] on the closely related trifluoromethyloxirane ($C_3H_3F_3O$) molecules, we made experimentally only the first step towards this ultimate goal: by fixing just one molecular-orientation axis

in space, we were able to demonstrate an enhancement of the PECD of uniaxially oriented chiral molecules up to about 10–20%.

Recently, we made the second step towards achieving the PECD of fixed-in-space chiral molecules [25]: we measured a polarization-averaged molecular-frame photoelectron angular distribution (MFPAD, [26,27]) of methyloxirane. Being emitted from a site- and element-specific core level, a photoelectron wave serves as a messenger of the molecular structure, providing the information on the target and on the dynamics of the process. Using these polarization-averaged MFPADs, we achieved an enantio-sensitive molecular structure determination with a bond-length resolution of about 5% for strong and even weak atomic scatterers alike [25]. However, such MFPADs are insensitive to the polarization state of the ionizing light, since all directions from which the light impinges onto the molecule are summed over. In the present work, we now exploit the sensitivity of photoelectron angular emission distributions to the helicity of circularly polarized light and, thus, make the final step to measure the differential PECD of a fixed-in-space methyloxirane molecule. Thereby, we demonstrate experimentally and theoretically that the normalized chiral asymmetry obtained as a function of two photoelectron emission angles and two molecular orientation angles can indeed exceed 50%.

The experimental data were recorded at beam line SEXTANTS of synchrotron SOLEIL, Saint-Aubin, France, and the experimental setup and conditions equal those reported in our previous works on methyloxirane [23,25]. The photoelectron energy of 550 eV was set to create O 1s photoelectrons with a kinetic energy of 11.5 ± 1.5 eV. The coincident detection of the momenta of charged ionic fragments and electrons was carried out by using a COLTRIMS reaction microscope [28,29]. We recorded the full data set for R- and S-enantiomers, as well as for light with positive and negative helicities (LCP and RCP), respectively. To ensure the same experimental conditions and minimize systematical errors, we toggled between LCP and RCP every two hours. To increase statistics, we combined results obtained for the two light helicities in the data analysis by applying the symmetry rules discussed below. Here, we present only the S-methyloxirane results, while Fig. S1 of the Supplemental Material [30] completes the full set of gathered data.

In order to determine the molecular orientation in space, three momentum vectors are required and thus only dissociation channels yielding at least three fragments can be considered. Here, we made use of our previous result [25] and chose so-called incomplete breakup channels: $C_3H_6O + \hbar\omega \rightarrow C_2H_{2,3}^+ + CH_2^+ + OH_{2,1}^0 + e_{ph}^- + e_{Aug}^-$. We constructed the fragment coordinate system as $\vec{Y} = \vec{p}_{C_2H_{2,3}^+}$, $\vec{Z} = \vec{p}_{C_2H_{2,3}^+} \times \vec{p}_{CH_2^+}$, and $\vec{X} = \vec{Y} \times \vec{Z}$. We discriminate the selected fragmentation channel from the

background by gating on a region in the photoion-photo-ion-coincidence spectrum and on specific intervals of the magnitude of the momenta of the two measured charged fragments and the third uncharged fragment. The momentum vector of the neutral fragment was computed from the measured momenta of the charged particles exploiting momentum conservation. The gates on the momenta were set to 45 a.u. $< |\vec{p}_{CH_2^+}| < 105$ a.u., 20 a.u. $< |\vec{p}_{C_2H_{2,3}^+}| <$ 110 a.u., and 20 a.u. $< |\vec{p}_{OH_{2,1}^0}|$. In addition, the condition on the minimum momentum of the neutral fragment ensured that the measured momenta of charged fragments are not colinear and thus define a plane. For fragments with several atoms, their center of charge does not necessarily coincide with their center of mass, which leads to the breakdown of the axial-recoil approximation [31]. Therefore, the fragment coordinate system, which is built on their detected asymptotic momenta, is slightly rotated with respect to the molecular coordinate system at the instant of photoionization. Details on finding such molecular coordinate system with the help of polarization-insensitive MFPADs can be found in our previous work [25]. Both the fragment (X, Y, Z) and the molecular (x', y', z') coordinate systems are illustrated in Fig. 1.

Our measured photoelectron emission distributions are depicted in the upper panels of Fig. 2 for different orientations of S-methyloxirane with respect to the direction of propagation of the RCP light. For a better representation, the distributions are shown as functions of the two emission angles (θ, φ) in the fragment (X, Y, Z) coordinate system (see Fig. 1). The light's propagation direction was also transformed in the fragment coordinates and is given by the same spherical angles. In order to increase statistics, the orientations from which the light hits the molecule were binned in 72 subsets in constant steps of
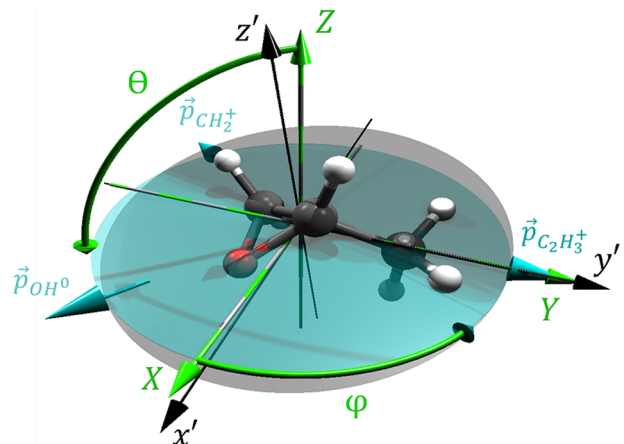

FIG. 1. Definition of the fragment coordinate system (green axes X, Y, and Z) for S-methyloxirane with the help of the asymptotic momenta of three fragments (turquoise arrows) together with the generated [25] molecular coordinate system at the instant of photoionization (black axes x', y', and z').
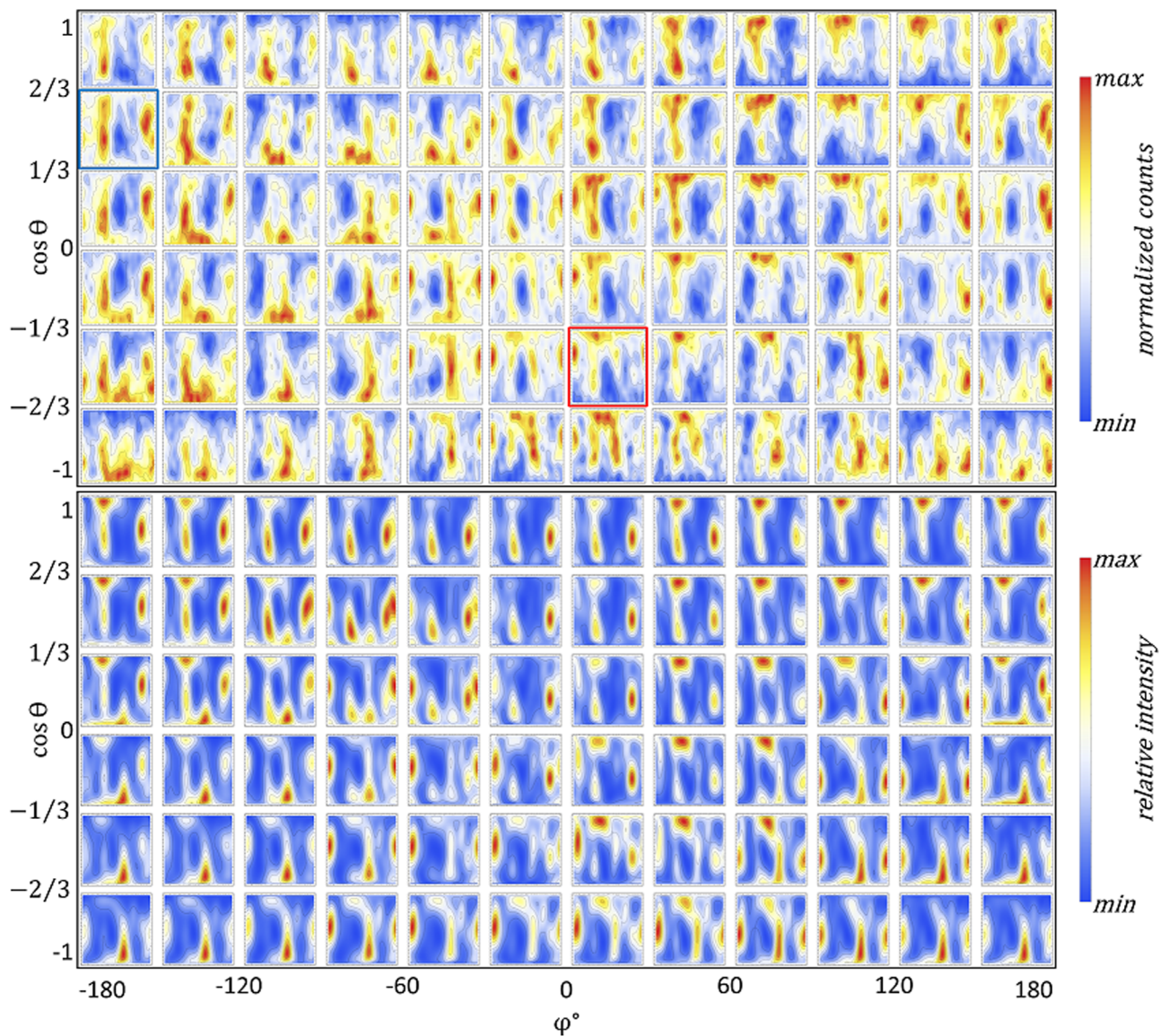
FIG. 2. Experimental (upper panels) and theoretical (lower panels) fourfold differential photoelectron emission distributions as functions of the photoelectron emission direction and the direction from which the RCP light hits the S-methyloxirane. Both directions are defined by spherical angles (θ, φ) given in the fragment (X, Y, Z) coordinate system as shown in Fig. 1. The location of each of the 72 patterns indicates the direction from which the light hits the molecule. In the electric-dipole approximation, a reversal of the direction of light in the fragment system is equivalent to a swap of the light helicity. Opposite directions are linked via transformations $\cos\theta \to -\cos\theta$ and $\varphi \to \varphi + 180°$. The positions of two panels highlighted by blue and red squares, which are shown in Fig. 3 on an enlarged scale, obey those transformations. Interchanging the enantiomers and light helicities mirrors the coordinate system via reflection at $\cos\theta = 0$ for the position of the panel and within each panel.

$\Delta\cos\theta = \frac{1}{3}$ and $\Delta\varphi = 30°$. Here, the position of each panel in the figure indicates the selected light propagation direction in the fragment coordinate system. A comparison of this representation for RCP with that for LCP light (see Fig. S1 of the Supplemental Material [30]) confirms the validity of the electric-dipole approximation. In this approximation, the light's electric-field vector is fully characterized by its sense of rotation [22]. An inversion of the light propagation direction in the fragment frame is, therefore, equivalent to an inversion of the light's helicity.

In Fig. 2, such an inversion of the light propagation direction corresponds to a selection of another panel, which is shifted as $\varphi \to \varphi + 180°$ and mirrored by $\cos\theta \to -\cos\theta$. Figure 2 illustrates a great sensitivity of the measured photoelectron emission distributions to the molecular orientation. This observation is fully confirmed by our *ab initio* calculations (see lower panels in the figure), performed by the single center (SC) method and code [32–34]. More details of the calculations can be found in our previous works [23,25,35] on this molecule.

A similar symmetry consideration links our measurements and calculations for S-methyloxirane, shown in Fig. 2, to those for R-methyloxirane. The fragment momenta define the turquoise plane in Fig. 1 and thus cannot determine the handedness of the coordinate system. Therefore, the reflection of the fragment coordinates at $\cos\theta = 0$ mediates switching between the two enantiomers together with the light helicities. This mirroring operation $\cos\theta \rightarrow -\cos\theta$ ought to be performed for both, the position of each panel in Fig. 2 (represents the light propagation direction) and the emission direction of the photoelectron in each panel. Figure S2 of the Supplemental Material [30] demonstrates this rule. Figure 3 illustrates the sensitivity of the photoelectron emission pattern obtained at a given molecular orientation to the helicity of the ionizing light. The selected molecular orientation is visualized in the insets. The experimental and theoretical emission distributions are depicted in two representations: as in Fig. 2 by the color maps and also via the three-dimensional polar representation (see caption of the figure for details). Such distributions can be understood as a three-dimensional diffraction pattern of the photoelectron wave, which originates at the oxygen atom and is multiply scattered on the chiral potential of methyloxirane. As one can see from this figure, being imprinted onto the emitted photoelectron waves, the helicity of the ionizing light influences the emission distributions dramatically. Both experiment and theory demonstrate rich structures and sizable contrasts between minima and maxima in the distributions, which are the main prerequisites for a strong circular dichroism effect.

We finally discuss the fourfold differential PECD of fixed-in-space S-methyloxirane, which is obtained as the normalized difference of the photoelectron emission distributions recorded for LCP and RCP light (indicated by I_+ and I_-), respectively: $\mathrm{PECD}(\theta, \varphi) = [I_+(\theta, \varphi) - I_-(\theta, \varphi)]/[I_+(\theta, \varphi) + I_-(\theta, \varphi)]$ [23,36]. This normalized difference refers to the dichroic parameter b_1, and not to the often-used $2b_1$ value [5–7]. The complete data set can be found in Fig. S3 of the Supplemental Material [30], where the present experimental and theoretical results are depicted in a way similar to that of Fig. 2. For the sake of brevity, we demonstrate here the fourfold differential PECD only for two selected molecular orientations (see Fig. 4 with the respective insets visualizing the chosen orientations). As one can see from Fig. 4, for some photoelectron emission directions, the measured fourfold differential PECD exceeds 50%. The measured PECD landscapes and signs are reproduced by our theory in great detail. However, the contrast of the computed PECD is somewhat larger than that of the measured one, well above 80%. This difference has a twofold origin. On the one hand, our fixed-nuclei calculations overestimate the chiral response, which is, in reality, washed out by the accompanying nuclear dynamics. On the other hand, the experiment underestimates the chiral
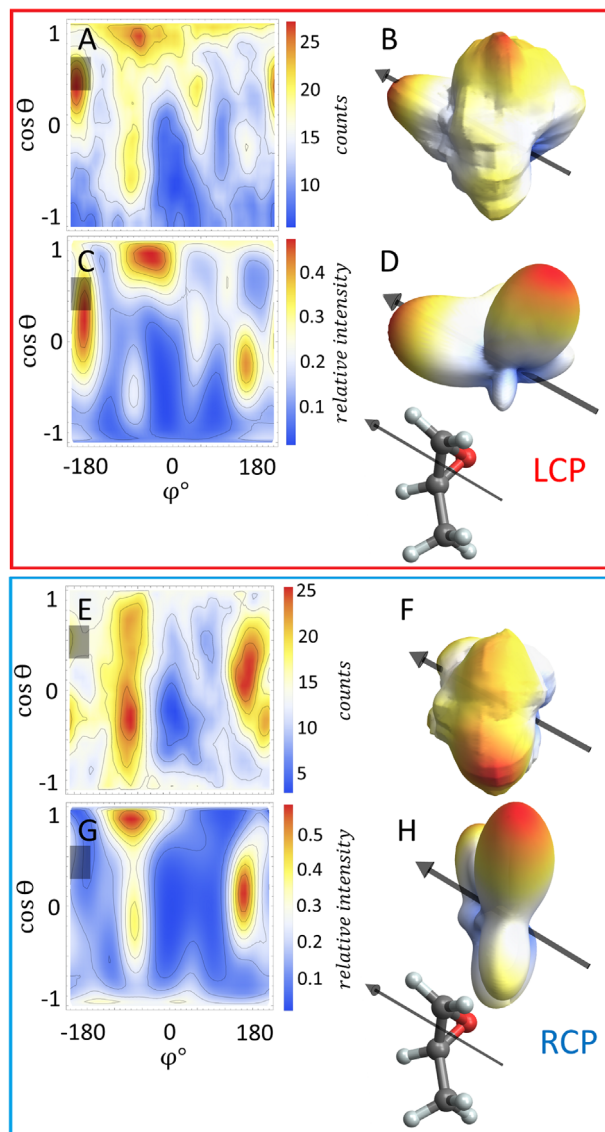

FIG. 3. Measured (a),(b),(e),(f) and computed (c),(d),(g),(h) photoelectron emission distributions in the fragment coordinate system for S-methyloxirane and LCP (a)–(d) or RCP (e)–(h) light under the condition that the light impinges from the direction indicated by the transparent gray squares [in (a),(c),(e),(g)] or gray arrows [in (b),(d),(f),(h)]. The red and blue borders around (a)–(d) and (e)–(h), respectively, highlight their locations in Fig. 2. The molecular orientation is also visualized in the insets. In panels (b), (d), (f), and (h), which depict the three-dimensional representation of the data from panels (a), (c), (e), and (g), respectively, the distance from the origin and the colour code indicate the number of emitted photoelectrons.

response. In the incomplete breakup channel used in the present analysis, momentum conservation allows us to access the momentum of the neutral fragment. It, hence, cannot anymore be used to better discriminate the chiral signal from the noise. In addition, variations in the fragmentation dynamics for the combined breakups with
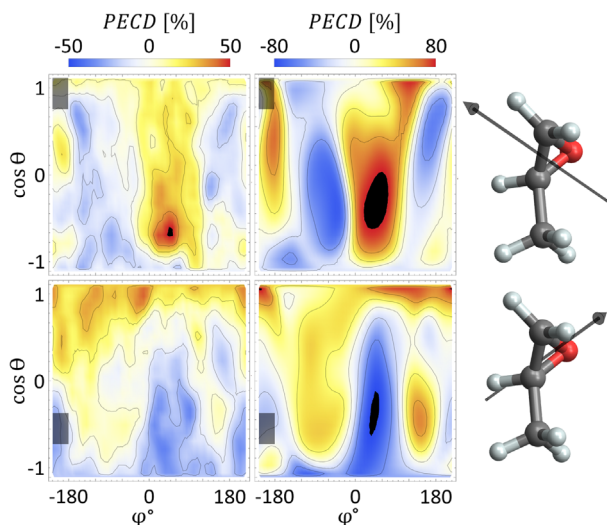
FIG. 4. Measured (left panels) and computed (right panels) fourfold differential PECDs for S-methyloxirane as functions of the two photoelectron emission angles for two different molecular orientations (light propagation directions), which are indicated by transparent gray squares and also by gray arrows in the respective insets. Black spots highlight photoemission directions at which the measured and computed PECDs exceed the presently chosen upper or lower limits of the respective asymmetry scales.

a proton attached to different fragments cause uncertainties in the determination of the fragment coordinate system.

In conclusion, we experimentally and theoretically studied the sensitivity of the O 1s photoelectron emission pattern of the chiral methyloxirane molecule to the helicity of circularly polarized light. We examined different orientations of the molecule with respect to the light propagation direction. Our measurements demonstrate that for distinct molecular orientations and photoelectron emission directions, the PECD can be enhanced above 50%. Taking into account that the measured and computed PECD strengths are also considerably reduced by the limited resolution in our determination of the molecular orientation (i.e., the binning of only 72 orientations in constant steps of $\Delta \cos \theta = \frac{1}{3}$ and $\Delta \varphi = 30°$), our results fully support the theoretical prediction of Ref. [23] that the differential PECD of a fixed-in-space chiral molecule can reach 100%. Such a strong asymmetry may allow for a chiral recognition of gaseous sample molecules with an unprecedented sensitivity.

* fehre@atom.uni-frankfurt.de
† schoeffler@atom.uni-frankfurt.de
‡ demekhin@physik.uni-kassel.de

[1] N. Berova, K. Nakanishi, and R. W. Woody, *Circular Dichroism: Principles and Applications* (Wiley, New York, NY, 2009).

[2] *Chiral Recognition in the Gas Phase*, edited by A. Zehnacker (CRC Press, Boca Raton, 2010).

[3] B. Ritchie, Phys. Rev. A **13**, 1411 (1976).

[4] N. Böwering, T. Lischke, B. Schmidtke, N. Müller, T. Khalil, and U. Heinzmann, Phys. Rev. Lett. **86**, 1187 (2001).

[5] I. Powis, Adv. Chem. Phys. **138**, 267 (2008).

[6] L. Nahon, G. A. Garcia, and I. Powis, J. Electron Spectrosc. Relat. Phenom. **204**, 322 (2015).

[7] S. Turchini, J. Phys. Condens. Matter **29**, 503001 (2017).

[8] S. Beaulieu, A. Ferré, R. Géneaux, R. Canonge, D. Descamps, B. Fabre, N. Fedorov, F. Légaré, S. Petit, T. Ruchon, V. Blanchet, Y. Mairesse, and B. Pons, New J. Phys. **18**, 102002 (2016).

[9] C. Lux, M. Wollenhaupt, T. Bolze, Q. Liang, J. Köhler, C. Sarpe, and T. Baumert, Angew. Chem., Int. Ed. Engl. **51**, 5001 (2012).

[10] C. S. Lehmann, N. B. Ram, I. Powis, and M. H. M. Janssen, J. Chem. Phys. **139**, 234307 (2013).

[11] C. Lux, A. Senftleben, C. Sarpe, M. Wollenhaupt, and T. Baumert, J. Phys. B **49**, 02LT01 (2016).

[12] K. Fehre, S. Eckart, M. Kunitski, C. Janke, D. Trabert, J. Rist, M. Weller, A. Hartung, M. Pitzer, L. Ph. H. Schmidt, T. Jahnke, R. Dörner, and M. S. Schöffler, Phys. Rev. Research **1**, 033045 (2019).

[13] S. Beaulieu, A. Comby, A. Clergerie, J. Caillat, D. Descamps, N. Dudovich, B. Fabre, R. Géneaux, F. Légaré, S. Petit, B. Pons, G. Porat, T. Ruchon, R. Taïeb, V. Blanchet, and Y. Mairesse, Science **358**, 1288 (2017).

[14] S. Beaulieu, A. Comby, D. Descamps, B. Fabre, G. A. Garcia, R. Géneaux, A. G. Harvey, F. Légaré, Z. Mašín, L. Nahon, A. F. Ordonez, S. Petit, B. Pons, Y. Mairesse, O. Smirnova, and V. Blanchet, Nat. Phys. **14,** 484 (2018).

[15] Ph. V. Demekhin, A. N. Artemyev, A. Kastner, and T. Baumert, Phys. Rev. Lett. **121,** 253201 (2018).

[16] S. Rozen, A. Comby, E. Bloch, S. Beauvarlet, D. Descamps, B. Fabre, S. Petit, V. Blanchet, B. Pons, N. Dudovich, and Y. Mairesse, Phys. Rev. X **9,** 031004 (2019).

[17] A. Kastner, C. Lux, T. Ring, S. Züllighoven, C. Sarpe, A. Senftleben, and T. Baumert, ChemPhysChem **17,** 1119 (2016).

[18] A. F. Ordonez and O. Smirnova, Phys. Rev. A **98,** 063428 (2018); **99,** 043416 (2019); **99,** 043417 (2019).

[19] R. E. Goetz, C. P. Koch, and L. Greenman, Phys. Rev. Lett. **122,** 013204 (2019).

[20] R. L. Dubs, S. N. Dixit, and V. McKoy, Phys. Rev. Lett. **54,** 1249 (1985).

[21] T. Jahnke, Th. Weber, A. L. Landers, A. Knapp, S. Schössler et al., Phys. Rev. Lett. **88,** 073002 (2002).

[22] A. Pier et al., Phys. Rev. Research **2,** 033209 (2020).

[23] M. Tia et al., J. Phys. Chem. Lett. **8,** 2780 (2017).

[24] G. Nalin et al., Phys. Chem. Chem. Phys. **23,** 17248 (2021).

[25] K. Fehre et al., arXiv:2101.03375.

[26] J. G. Underwood and K. L. Reid, J. Chem. Phys. **113,** 1067 (2000).

[27] A. Landers et al., Phys. Rev. Lett. **87,** 013002 (2001).

[28] R. Dörner, V. Mergel, O. Jagutzki, L. Spielberger, J. Ullrich, R. Moshammer, and H. Schmidt-Böcking, Phys. Rep. **330,** 95 (2000).

[29] J. Ullrich, R. Moshammer, A. Dorn, R. Dörner, L. Ph. H. Schmidt, and H. Schmidt-Böcking, Rep. Prog. Phys. **66,** 1463 (2003).

[30] See the Supplemental Material at http://link.aps.org/supplemental/10.1103/PhysRevLett.127.103201 for a full account of the experimental and theoretical data, which includes Figs. S1–S3.

[31] R. N. Zare, Mol. Photochem. **4,** 1 (1972).

[32] Ph. V. Demekhin, D. V. Omel'yanenko, B. M. Lagutin, V. L. Sukhorukov, L. Werner, A. Ehresmann, K.-H. Schartner, and H. Schmoranzer, Opt. Spectrosc. **102,** 318 (2007).

[33] Ph. V. Demekhin, A. Ehresmann, and V. L. Sukhorukov, J. Chem. Phys. **134,** 024113 (2011).

[34] S. A. Galitskiy, A. N. Artemyev, K. Jänkälä, B. M. Lagutin, and Ph. V. Demekhin, J. Chem. Phys. **142,** 034306 (2015).

[35] G. Hartmann et al., Phys. Rev. Lett. **123,** 043202 (2019).

[36] U. Hergenhahn, E. E. Rennie, O. Kugeler, S. Marburger, T. Lischke, I. Powis, and G. A. Garcia, J. Chem. Phys. **120,** 4553 (2004).